

Translated by J. G. Adashko

Nonstationary Josephson effect at a point junction under high voltage

Kh. A. Aĭnitdinov, S. I. Borovitskii, and L. L. Malinovskii

(Submitted 22 September 1978)

Zh. Eksp. Teor. Fiz. **76**, 1342-1350 (April 1979)

The behavior of the Josephson current steps observed at high microwave potentials and powers in the case of a new type of clamped point junction is explained. It is concluded that at junctions consisting of metallic bridges which are small (of size d) compared with the coherence length (ξ_0) and mean free path (l), the phase dependence of the nonstationary Josephson current is sinusoidal. The formation of the current step is restricted by the heating of the junction at high voltages. The limiting voltage is $V_h \sim (l/d)^{1/2}$. For the Nb-Nb junctions studied, Josephson steps up to 14 mV have been obtained.

PACS numbers: 74.50. + r, 85.25. + k

INTRODUCTION

At a voltage above the energy gap of a superconductor $eV > 2\Delta_0$, the nonstationary Josephson effect at tunnel junctions has been observed experimentally by Hamilton¹ and described theoretically by Werthamer² and by Larkin and Ovchinnikov.³ The height of the current step induced by microwaves was calculated earlier.⁴ The most remote steps in voltage at a tunnel junction have been observed by McDonald *et al.*⁵ No description has been made of the behavior of point junctions at voltages beyond the gap value, although there is interest both in the theory and in the practical utilization (for example, as a voltage standard).

In the present work we set forth the results of an experimental study of the characteristics of a clamped Josephson point junction of a new type in a microwave field, and explain it on the basis of a proposed microscopic theory of a bridge of dimensions less than $\{l, \xi_0\}$. From a comparison of the measured dependence of the height of the induced steps on the microwave amplitude with the theoretical value, it is concluded that the phase of the nonstationary Josephson current has a sinusoidal dependence on the phase in the investigated junctions. The dependence of the current step height I_N at the upper voltage limit on its value V_N has an asymptotic form: $I_N(V_N) \sim V_N^{-1/3}$. Preliminary results of the research were reported earlier.⁶

DESCRIPTION OF THE JUNCTION

The experiments were carried out with clamped Nb-Nb junctions, which were prepared under room conditions and which did not change their characteristics

after numerous coolings to the temperature of liquid helium ($T = 4.2$ K). The junction shown schematically in Fig. 1 comprises a wire electrode in the form of a loop pressed to a flat electrode. The flat screen-electrode was made of single-crystal Nb and its surface was carefully smoothed by electrochemical polishing. The surface of the niobium loop was cleansed from foreign impurities and oxides by chemical etching.

A trace of the loop with overall dimension $5 \times 100 \mu$ is seen on a microphotograph of the screen, obtained by means of a scanning electron microscope after dismantling the junction. It can be assumed that a set of microbridges is formed on this area, distributed in correspondence with the very inhomogeneous microstructure of the wire surface. The total resistance of the junction is the combination of the resistances of the microbridges connected in parallel.

In correspondence with this model, the average diameter of the microbridges was determined from the measurements of the dependence of the resistance of the junction on the temperature $R(T)$ and voltage $R(V)$. The measurement of $R(T)$ and $R(V)$ was carried out in a thermostat in which the temperature was maintained and measured accurate to ~ 1 in the range 12-300 K. The dependence $R(V) = dV/dI$ was determined from the value $\bar{V} - IR(0)$, measured with the help of a bridge

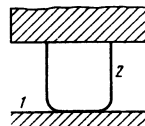


FIG. 1. Schematic diagram of the clamped point Josephson junction of the new type: 1—plane electrode-screen, 2—wire electrode-loop.

circuit⁷; here \bar{I} and \bar{V} are the dc current and the voltage at the junction, and $R(0)$ is the initial ($\bar{V}=0$) resistance of the junction. The measurement of $R(\bar{V})$ was made with accuracy $\sim 0.1\%$ in the voltage range 0–100 mV.

The junctions divide into two types, depending on the forms of $R(T)$ and $R(\bar{V})$ (Figs. 2, 3). The resistance of some junctions (curves 2, 3 Fig. 2) increases linearly just as the resistivity of the niobium wire $\rho(T)$ (curve 4, Fig. 2) upon increase in the temperature in the range 25–300 K, while the dependence $\bar{V}-\bar{I}R(0)$ on \bar{V} is parabolic at $\bar{V} \geq 15$ mV (curve 1, Fig. 3). Such a behavior is characteristic for metal bridges of dimensions much greater than atomic.⁸ For the normal resistance of a single bridge of size d , we have the interpolation formula⁹

$$R = \frac{2\rho l}{\pi d} \left(\frac{2}{d} + \frac{1}{l(T)} \right), \quad (1)$$

where $\rho(T)l(T)$ is a constant independent of the temperature ($\approx 4 \times 10^{-12}$ ohm-cm² for Nb), $l(T)$ is the mean free path of the electrons in the metal. The function (1) was checked against the $R(T)$ dependence, measured on specially prepared junctions with a single bridge. In the case of junctions made up of a set of parallel-connected microbridges, the mean diameter of the microbridges \bar{d} was obtained from the slope of curves 2 and 3 in Fig. 2 according to formula (1). For our junctions, \bar{d} was in the range 10–100 Å.

In junctions of the second type, the dependence $R(T)$ departs from a linear one at $T \geq 100$ K (curve 1, Fig. 2), and $R(\bar{V})$ falls off at $\bar{V} \geq 15$ mV (curve 2, Fig. 3). These features were most sharply pronounced in junctions prepared without chemical cleaning of the Nb electrodes or when they are specially cleaned by heating in air ($T \leq 200$ °C). Such junctions are not SIS tunnel junctions, since the volt-ampere characteristics (VAC) on them have no gap singularity. Transition to the second type takes place also with clean junctions upon decrease in the diameter of the bridges. The singularities of junctions of the second type can be explained by the presence in the junction of portions that are in contact through

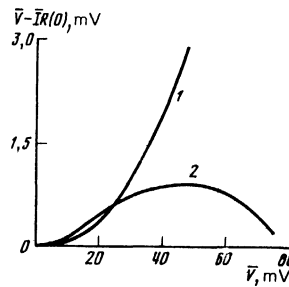


FIG. 3. Recording, obtained with a bridge circuit, of two types of the $\bar{V}-\bar{I}R(0)$ dependence for junctions in the normal state ($T=12$ K): 1—for a pure junction; 2—for a junction with sections that make contact through the potential barrier.

the potential barrier for low-energy electrons, contacts produced because of the difference in electron concentrations at the boundary between pure Nb and its metallic oxides or in a bridge of dimensions comparable with atomic dimensions.

EXPERIMENTAL RESULTS AND COMPARISON WITH THEORY

For subsequent study, we chose junctions of the first type only. Figure 4 shows the $\bar{I}R(0)-\bar{V}$ dependences obtained for such junctions in the superconducting state ($T=4.2$ K). A bend is observed on the graphs, the location of which depends on the conductivity of the wire electrode of the junction. For a wire with low conductivity ($l(10) \approx 20-40$ Å) the bend is located at a voltage of $V_h = 1-2$ mV (curve 1, Fig. 3) while in purer materials ($l(10) \approx 400$ Å) this bend is shifted toward higher voltages (curves 2 and 3, Fig. 4). The location of the bend also depends on the diameter of the microbridges of the junction. The bend is explained by the warming up of the individual microbridges of the contact and their transition to the normal state. It has been shown⁴ that the heating voltage $V_h \sim (l/d)^{1/2}$ at $d < l$ and $V_h = \text{const}$ at $d > l$.

The VAC of the junctions were obtained with an oscilloscope in the given-current regime. Figure 5a shows

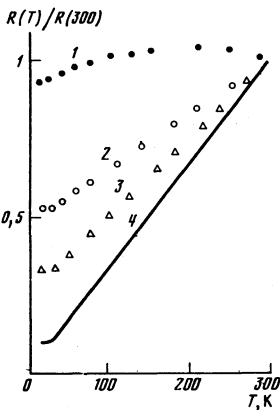


FIG. 2. Temperature dependence of the normal resistance $R(T)$ of two junctions (curves 1 and 2) on the boundary of the resistance region (0.1–0.3 ohm), used for obtaining the current steps at high potentials; ●—curve 1, ○—curve 2, △—curve 3. The solid line 4 denotes the dependence of the resistivity $\rho(T)$ of niobium wire.

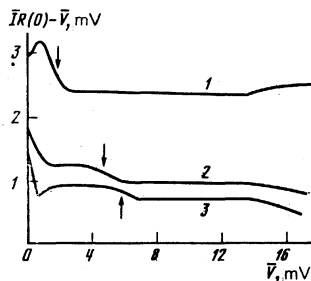


FIG. 4. Bridge-circuit plots of $\bar{I}R(0)-\bar{V}$ in the superconducting region ($T=4.2$ K) for junctions with different diameter bridges, made of materials with different purity; 1—for a junction with a wire electrode of Nb+50% Zr ($l(10)=20$ Å), $20 \text{ Å} \leq d \leq 100 \text{ Å}$; 2, 3—for junctions with a wire electrode of pure Nb ($l(10)=400$ Å), $d_2=200$ Å, $d_3=80$ Å. The arrows on the plots indicate the positions of thermal heating V_h . At a potential of ≈ 16 mV, a bend is observed in curve 1, corresponding to the first maximum of the density of phonon states of Nb.

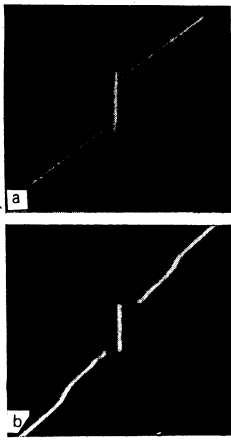


FIG. 5. Oscillograms of two types of VAC for pure junctions: a—junction with $R(T)$ dependence of the first type, $d=90 \text{ \AA}$; b—junction with $R(T)$ dependence of the second type, $d=20 \text{ \AA}$. scales: along the horizontal—2 mV/cm (a,b), along the vertical 23.5 mA/cm (a) and 8.7 mA/cm (b).

an oscillogram of a typical VAC. The presence of an excess current,¹⁰ the absence of a gap singularity, and hysteresis near zero voltage are typical of this VAC. As \bar{d} (the slope of $R(T)$) decreases the $R(T)$ dependence of the first type undergoes a continuous transition to that of the second type and a significant increase of the superconducting current at $eV = 2\Delta_0$ —the gap singularity—is observed on the VAC (Fig. 5b).

In the study of nonstationary characteristics, the junction is placed at the antinode of the electric field of a coaxial resonator. The radiation is introduced by means of a standard klystron oscillator with frequency $\omega_0 \approx 10 \text{ GHz}$. The Josephson current steps at a voltage $V_N = N\hbar\omega_0/2e$ was measured on the screen of an oscilloscope at an amplitude 0.1–1 mV of the alternating (50 Hz) sweep and a dc junction bias in the range 0–15 mV. Typical oscillograms of the stepped VAC are shown in Fig. 6.

The current steps vanish at a specified microwave current amplitude \bar{I} when the bias voltage exceeds $\bar{I}R$. With decrease in the voltage to the value $\bar{I}R$, the steps increase rapidly in size, after which their height

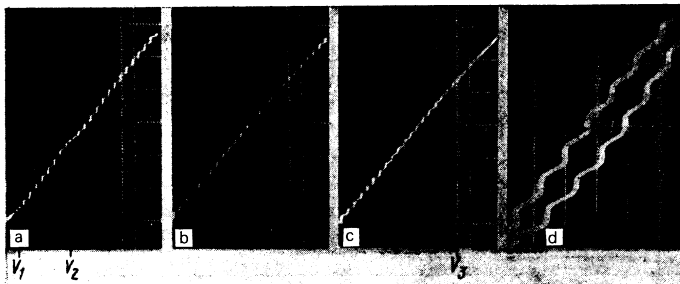


FIG. 6. Oscillogram of a portion of stepped VAC at fixed microwave power, containing the first wide and the last narrow groups of current steps: a—narrow group (at the bottom of the frame) and the beginning of the broad group, b—continuation of the broad group; c—end of the broad group; V_1 and V_2 are the beginning and end of the narrow group, V_3 is the upper boundary of the broad group. Here $V_3 = 3.1 \text{ mV}$, $I_0(0)R = 1 \text{ mV}$. The scale along the vertical is 1 mA/cm, along the horizontal, 100 $\mu\text{V}/\text{cm}$; d—current steps in large scale (100 $\mu\text{A}/\text{cm}$, 25 $\mu\text{V}/\text{cm}$) at a displacement voltage of $V_N = 10 \text{ mV}$. The oscillogram d is taken on the same junction at higher microwave power than in a, b, c.

changes weakly over a wide range of voltages containing a group of 40–80 steps, depending on the value of the excess current (first group). Then the height of the steps falls off rapidly and upon further decrease in the bias it oscillates with a period of the Bessel function according to its index ($\approx N^{1/3}$). The height of the current steps I_N at the upper boundary of the wide group, where $V_N = \bar{I}R$, was measured as a function of change in the microwave power. In Fig. 7, the circles and crosses indicate the experimental results of the measurements of the $I_N(V_N)$ dependence. For all the junctions, this dependence was the same slowly decreasing function of V up to the thermal heating voltages V_h (Fig. 4). For voltages above V_h , the decrease of $I_N(V_N)$ becomes steeper (crosses on Fig. 7). The measurements were carried out at a background level $\approx 5\mu\text{V} - R^{-1}$, which is connected with the instability of the microwave power at the junction. Even at such a background level, steps up to 14 mV were observed at individual junctions. This approaches the maximum voltage step $\approx 15 \text{ mV}$ obtained in the work of MacDonald *et al.*⁵ on a mechanically adjustable Nb–Nb junction, where a complicated technique of averaging was used to separate the current steps of $I_N \leq 1 \mu\text{A}$ from the background.

A calculation of the density of the nonstationary Josephson current in a bridge with dimensions less than $\{l, \xi_0\}$ but much greater than the dimensions of the atomic lattice was made to explain the experimental characteristics of the junction. The calculation was based on the fact that in the region of falloff of the bridge voltage the order parameter $\Delta(r, t) = 0$. In this region, the current density exceeds the critical value. As a result of the solution of the boundary-value problem for the basic equations of a pure superconductor¹¹ with the boundaries given in Ref. 12, the following expression is obtained for the current density at the center of the bridge:

$$j(t) = j_n + j_e + \text{Im} \left\{ j_s(V) \exp \left(i \frac{2e}{\hbar} \int V(t) dt \right) \right\}, \quad (2)$$

where $V(t)$ is the total voltage drop on the bridge; it changes slowly (in the scale Δ_0^{-1}) with time. The amplitude of the Josephson current at $T = 0$ has the form

$$j_s(V) = \frac{4\Delta_0^2}{e\phi l} i \int_0^\infty \frac{d\omega}{[\omega + eV + ((\omega + eV)^2 - \Delta_0^2)^{1/2}][\omega + (\omega^2 - \Delta_0^2)^{1/2}]}. \quad (3)$$

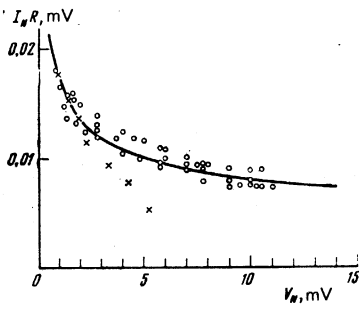


FIG. 7. Dependence of the height of the current step I_N at the upper boundary of the voltage on its value V_N . The continuous curve corresponds to the dependence $I_N(V_N) \sim (V_N)^{-1/2}$. The crosses \times indicate the experimental data for a junction with thermal heating.

In particular,

$$j_s(0) = 8\Delta_0/3e\rho l;$$

at $eV \gg \Delta_0$,

$$j_s(V) = \left[\pi + i \left(1 + 2 \ln \frac{2V}{\Delta_0} \right) \right] \frac{\Delta_0^2}{2e^2 V \rho l}.$$

Plots of $\text{Re}j_s(V)$, $\text{Im}j_s(V)$, $|j_s(V)|$ are given in Fig. 8. The characteristic scale of the change in $j_s(V)$ for the microbridge is Δ_0 .

The excess-current density in (2) is equal to

$$j_e(V) = \frac{2\Delta_0 \langle \varphi_1 - \varphi_2 \rangle}{e\rho l} \left[\frac{2}{3} - \text{Im} \int_{eV}^{\infty} \frac{\Delta_0 d\omega}{[\omega + (\omega^2 - \Delta_0^2)^{1/2}]^2} \right], \quad (4)$$

where

$$\langle \varphi_1 - \varphi_2 \rangle = \frac{i}{2} \Delta_0^{-2} \int_{-\infty}^{+\infty} \left(\Delta \frac{\partial \Delta^*}{\partial r} - \Delta^* \frac{\partial \Delta}{\partial r} \right) dr.$$

The normal component $j_n(V) = V/\rho l$ of the current density in (2) differs from zero over the entire range of values of $V(\rho l = 4p_F/3n_0e^2)$, where p_F is the Fermi momentum, n_0 is the concentration of electrons in the metal).

The VAC of a microbridge in the given-current regime for $\bar{V} > 0$, calculated from (2), has the form

$$I(\bar{V}) = [I_s^2(\bar{V}) + (\bar{V}/R)^2]^{1/2} + I_e(\bar{V}), \quad (5)$$

where the total currents I , I_s and I_e are equal to the corresponding densities multiplied by the cross section area of the bridge. A plot of $I(\bar{V})$ is shown in Fig. 9. The characteristic features of the theoretical VAC, as well as those of the experimental ones (see Fig. 5), are the presence of the excess current I_e and the hysteresis of $I(\bar{V})$ near zero voltage. The latter is connected with

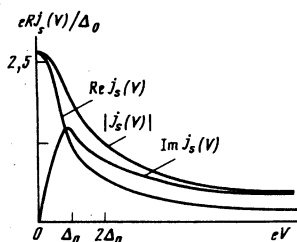


FIG. 8. Real and imaginary parts of the amplitude of the Josephson current density $j_s(V)$ at $T=0$.

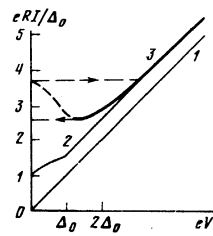


FIG. 9. Theoretical (5) VAC of a bridge in the specified current regime: 1—VAC of the bridge in the normal state, 2—plot of $\bar{V}/R + I_e(\bar{V})$, 3—VAC of a bridge in the superconducting state. The arrows indicate the direct and reverse branches of the hysteresis loop.

the smaller value of the amplitude of the Josephson current $I_s(\bar{V})$ at finite values of the voltage in comparison with $I_s(0)$. The coefficient $\langle \varphi_1 - \varphi_2 \rangle \approx 3/8$ is determined from the experimental VAC for I_e from (4).

Zimmerman observed similar characteristics on "perfectly pure" junctions of Nb-Nb,¹³ and Yanson¹⁴ observed them on indium microbridges obtained by breakdown of film structure. At junction resistances below 10–20 ohms, the experimental VAC¹³ is completely identical also in the numerical coefficients with the theoretical one (5). Even in the case in which such a junction is a single bridge, its diameter, calculated from (1), cannot exceed 70 Å, which is much smaller than ξ_0 (≈ 400 Å for Nb), i.e., the conditions for application of the formula (5) are satisfied. We note that on such junctions, gap singularities are absent both in experiment and in the proposed theory.

On the basis of the expression (2), we calculate the height of the current step at constant voltage $V_N = N\hbar\omega_0/2e$, induced under the microwave action ($\omega_0 < \Delta_0$). The calculation is carried out in the given-current regime $I(t) = \bar{I} + \bar{I} \cos \omega_0 t$, which obtains in our measurements (the resistance of the junction is small in comparison with the external impedance) under the following conditions: $\bar{I} > I_e(0)$, $I_e > I_s$. Upon neglect of I_s , the VAC is written down in the following form in the presence of microwaves:

$$\bar{V} = (\bar{I} - I_n)R + \left[\frac{\hbar\omega_0}{2e\pi} \Phi_- - (\bar{I} - I_e)R\theta(\bar{I} - \bar{I} + I_e) \right] - \left[\frac{\hbar\omega_0}{2e\pi} \Phi_+ - (\bar{I} + I_e)R\theta(\bar{I} - \bar{I} - I_e) \right], \quad (6)$$

where

$$\Phi_{\pm} = \frac{2eR}{\hbar\omega_0} [I \cos \omega_0 t_{\pm} + \omega_0 t_{\pm} (\bar{I} \mp I_e)] \theta(\bar{I} - \bar{I} \pm I_e),$$

$$\omega_0 t_{\pm} = \arccos \frac{\pm I_e - \bar{I}}{\bar{I}}, \quad \theta(x) = \begin{cases} 1 & \text{at } x > 0 \\ 0 & \text{at } x < 0 \end{cases}.$$

In the first approximation in I_s we obtain for the height of the induced current step:

$$I_N \approx I_s(0) \frac{2}{\pi} \left| \int_0^{\pi} dt [1 - \theta(t - t_-) \theta(t_+ - t)] \cos \frac{2eR}{\hbar} \times \int_0^t dt I(t) \left(1 - \left| \frac{I_e}{\bar{I}} \right| \right) \theta \left(1 - \left| \frac{I_e}{\bar{I}} \right| \right) \right|. \quad (7)$$

If $2eI_N R/\hbar\omega_0 < 1$, we can limit ourselves to the first approximation. The integral in (7) is approximated in the following fashion:

$$I_N \approx I_s(0) |J_{p-\alpha}(\bar{A}) + \operatorname{Re}[e^{i(\Phi_0 - \Phi)} H_{p+\alpha}^{(1)}(\bar{A})]|, \quad (8)$$

where

$$p = 2e\bar{I}R/\hbar\omega_0, \quad \alpha = 2eI_e R/\hbar\omega_0, \quad \bar{A} = 2eTR/\hbar\omega_0;$$

$J_p(x)$ and $H_p^{(1)}(x)$ are the Bessel and Hankel functions, respectively. The numerical solution of the differential equation (2) on a computer agrees with the calculation according to Eq. (7).

It follows from (7) that the first broad group of current steps occupies the region of constant currents $\bar{I} - I_e \leq \bar{I} \leq \bar{I} + I_e$, which contains

$$\delta N = \frac{4eI_e R}{\hbar\omega_0} \left(1 - \frac{2}{\pi} \left(\frac{I_e}{\bar{I}}\right)^{1/2}\right)$$

steps. This describes the already noted singularity of the stepwise experimental VAC connected with the excess current. In the experiment, $I_e(0)R \approx 0.5 - 1$ mV, which corresponds to $\delta N \approx 40 - 80$, i.e., it is identical with the measured width of the first group. In the absence of an excess current (tunnel junction), the first group contains only $\approx N^{1/3}$ steps. For the height of the current step in the upper slope of the first group $\bar{I} = \bar{I} + I_e$ the following approximate formula holds:

$$I_N \approx 0.9I_s(0) (\hbar\omega_0/2eV_N)^{1/2}. \quad (9)$$

The experimental points $I_N(V_N)$ shown in Fig. 7 are close to the theoretical curve (9).

For a test of the conclusion of the theory (2) as to the sinusoidal character of the phase dependence of the nonstationary Josephson current, we measured the dependence of the height of the null current step I_0 on the microwave power. If we permit a deviation from sinusoidal dependence in the form of $j(\varphi) = j_1 \sin\varphi + j_2 \sin 2\varphi$, then the null step is described by the expression [similar to (7)] $\delta I \sim j_1 \cos(\Phi_0 - \pi/4) \sin\varphi_0 + 2^{-1/2} j_2 \cos(2\Phi_0 - \pi/4) \sin 2\varphi_0$, where φ_0 is the initial phase difference. It is then seen that if $j_2 \neq 0$, then $I_0 \neq 0$ no matter what the value of \bar{I} . Junctions with $R \geq 0.1$ ohm were chosen for the measurements. Subharmonic steps were absent on the VAC of such junctions, and the height of the null step vanished at certain \bar{I} accurate $\approx 1 \mu V - R^{-1}$. Consequently, $j_2 < 0.1j_1$, i.e., $\sin\varphi$ holds at the measurement accuracy achieved in the experiment.

A value $I_s \approx 0.1$ mV $- R^{-1}$ was obtained from the measurements of $I_N(V_N)$ (see Fig. 7) for the amplitude of the sinusoidal component of the Josephson current. This value is smaller than the theoretical (3). The smallness of I_s , and also the deviation difference from the theory in the initial section of the return path of the hysteresis plot of $I(\bar{V})$ can be attributed to the interaction of the electrons with the lattice vibrations, which are intense in the narrowing region. The latter result is attested by the experimental⁹ plot of $R(\bar{V})$ of small bridges in the normal state, since this plot shows singularities of the spectral density of the phonon states of the metal. Allowance for electron scattering by the lattice vibration in the correlation function $G(\mathbf{r}_1, t_1; \mathbf{r}_2, t_2)$ in the narrowing region greatly reduces the absolute value of $j_s(V)$ and changes the second component for $j_e(V)$ in (4). The bridge resistance R changes little, since the wave vec-

tor of the lattice vibrations is perpendicular to the electron current. To test this assumption, we need additional experiments on individual bridges of materials of different purity.

Thus the proposed microscopic theory of bridges of small dimensions can serve as the basis of an additional study of their properties.

CONCLUSION

The sinusoidal character of the phase dependence of the nonstationary Josephson current, obtained in the theory (2), is proved experimentally by measurements $I_0(\bar{I})$. The $I_N(V_N)$ dependence, first recorded at the point junction at above-gap voltages, is excellently described by the theory (7), (8), but differs from the known dependence for tunnel junctions.^{1,4} This difference is attributed by the proposed theory to the fact that the total junction current contains besides the normal and sinusoidal components also the excess current. On the basis of the investigations that have been carried out, we can draw the following conclusions:

1. The obtaining of Josephson steps far from the gap is connected with the smallness of the bridge dimensions in comparison with l and ξ_0 .
2. The limiting voltage of the current steps is set by the thermal heating of the bridges under the action of the applied voltage. The parameter determining the heating of the bridge is the quantity l/d .
3. In the preparation of the junctions, it is necessary to use pure materials with high thermal conductivity and to strive for the use of the finest grained structure of the junction electrodes.

For practical use, particularly for an effective amplification and shift of the microwaves to the infrared region, it is important that the height of the steps in the VAC of the junction decrease slowly with increase in the voltage: $I_N(V_N) \sim (V_N)^{-1/2}$. We note that the longevity of the construction and the simplicity of the technology of preparation of the junction of the new type enables us to broaden considerably the region of application of the Josephson effect.

The authors thank I. K. Yanson for useful discussion of the research.

¹C. A. Hamilton, Phys. Rev. B5, 912 (1972).

²N. R. Werthamer, Phys. Rev. 147, 255 (1966).

³A. I. Larkin and Yu. N. Ovchinnikov, Zh. Eksp. Teor. Fiz. 51, 1535 (1966) [Sov. Phys. JETP 24, 1035 (1967)].

⁴S. I. Borovitskiĭ and L. L. Malinovskii, Radiotekhnika i elektronika 20, 147 (1975).

⁵D. G. McDonald *et al.*, Appl. Phys. Lett. 15, 121 (1969).

⁶Kh. A. Aĭnitdinov, S. I. Borovitskiĭ, and L. L. Malinovskii, Papers at the XIX All-union conference on low temperature physics (LT-19) Minsk, September, 1976, p. 376.

⁷A. I. Akimenko, V. S. Solov'ev and I. K. Yanson, Fiz. Nizk. Temp. 2, 480 (1976) [Sov. J. Low Temp. Phys. 2, 238 (1976)].

⁸N. I. Bogatina and I. K. Yanson, Zh. Eksp. Teor. Fiz. 63, 1312 (1972) [Sov. Phys. JETP 36, 692 (1973)].

⁹I. K. Yanson, Zh. Eksp. Teor. Fiz. 66, 10 35 (1974) [Sov. Phys.

¹⁰J. I. Pankov, Proceedings (Trudy) of the X International conference on low temperature physics, Moscow, 1966, p. 257.

¹¹A. A. Abrikosov, O. P. Gor'kov and I. E. Dzyaloshinskii, *Metody kvantovoi teorii polya v statisticheskoi fizike* (Quantum Field Theoretical Methods in Statistical Physics), Fizmatgiz, 1962 [Pergamon, 1965].

¹²O. Iwanyshyn and H. I. I. Smith, *Phys. Rev.* B6, 121 (1972).

¹³J. E. Zimmerman, *Proc. Appl. Supercond. Conf. Annapolis*, PIII, 552 (1972).

¹⁴I. K. Yanson, *Fiz. Nizk. Temp.* 1, 141 (1975) *Sov. J. Low Temp. Phys.* 1, 67 (1967)].

Translated by R. T. Beyer

Elastic properties of cerium at pressures up to 84 kbar and at a temperature of 293 K

F. F. Voronov, V. A. Goncharova, and O. V. Stal'gorova

Institute of High Pressure Physics, Academy of Sciences USSR

(Submitted 27 September 1978)

Zh. Eksp. Teor. Fiz. 76, 1351-1356 (April, 1979)

The elastic properties of polycrystalline cerium have been studied by the ultrasonic method under conditions of quasihydrostatic pressures up to 84 kbar at a temperature of 293 K. The pressure dependence of the density, elastic bulk modulus, shear modulus and Debye temperature were determined from the data obtained on the velocities of propagation of longitudinal and transverse ultrasonic waves. An anomalous change in a number of elastic characteristics were observed, connected with the γ - α (7.5 kbar) and α - α' (51 kbar) phase transformations. The singularities of the change in the elastic properties of the α - and α' - phases of cerium point to a structural character of the α - α' transformation. It follows from an estimate of the dependence of the density on the pressure that the most probable structure of the α' - phase of cerium is orthorhombic of the α - uranium type. A softening of the longitudinal acoustical modes was observed upon approach to the electronic γ - α transition and a softening of the transverse acoustical modes upon approach to the structural α - α' transformation. The softening of the phonon spectrum of cerium found at high pressures correlates with the superconductivity phenomenon, and explains also the singularities of the melting curve of cerium in correspondence with Lindemann's representations.

PACS numbers: 62.20.Dc, 43.35.+d, 63.20.Dj

At high pressures, cerium exhibits a number of interesting properties, due to a change both in the electronic states and in the symmetry of the lattice. The anomalous increase in the compressibility of the γ phase of cerium with pressure is well known, as is the jumpwise decrease in the volume of the face-centered cubic (FCC) lattice by 14% at 7.5 kbar.¹ It has been shown that the localized 4f electron goes in this case to the *sd* conduction band,² and the magnetic FCC (the γ phase of cerium) goes over into the nonmagnetic FCC (the α phase).³ The equilibrium line of the γ - α transformation terminates at the critical point.⁴ It follows from measurements of the Hall effect⁵ that the number of 4f electrons decreases by 0.6-0.8 in the γ - α transition, while the valence changes from 3.06 ± 0.06 to 3.67 ± 0.09 .⁶ It has been suggested¹ that further compression increases the valence of α -Ce to 4.0; however, neutron diffraction analyses⁷ have shown that the 4f electron becomes delocalized already at 8 kbar.⁸ At 51 kbar, as was noted from the jump in the electrical resistance,⁹ α -Ce transforms into α' -Ce; the equilibrium line of this transformation was determined in Ref. 10. It was found that α' -Ce is superconducting.^{8,11} On the basis of x-ray investigations, various structures were proposed for the α' -phase: FCC,¹² slightly distorted HCP,¹³ orthorhombic of α -uranium type,¹ HCP,¹⁴ and corres-

pondingly various volume discontinuities in the α - α' transition. X-ray structure in investigations up to 175 kbar¹⁵ have shown the existence of a tetragonal phase of cerium above 120 kbar; however, the structure of the α' phase was not interpreted in that work. The sharp change in the slope of the plot of the electrical resistance of cerium on the pressure in this transition has been proposed as a reference point of the pressure scale.¹⁶

There is undoubted interest in the study of the propagation velocity of elastic waves in cerium over a wide range of pressures. These reflect the changes in the low-frequency acoustic part of the phonon spectrum and determine the elastic characteristics of the high pressure phases and the features of their change as a result of phase transitions.

The elastic characteristics of cerium were studied by us previously up to 9 kbar,¹⁷ and we first observed the strong softening of the longitudinal acoustic modes near the γ - α transformation.

For the present experimental investigations, we used polycrystalline cerium of grade TseM-1 with content of the basic ingredient 99.93%, of grade Ce É-1 (99.53%), and cerium of purity 99.95% obtained from the CNRS